Simulation Study of a Heuristic Predictive Optimization Scheme for Grid-Reactive Heat Pump Operation

Tillman Faßnacht[1], Manuel Loesch[2], Andreas Wagner[3],

[1,3]*Karlsruhe Institute of Technology, Building Science Group*, [2]*FZI Research Center for Information Technology*

Abstract – **A heuristic predictive optimization scheme for grid-reactive heat pump operation is introduced in this paper. It is based on thermal demand predictions (domestic hot water, heating demand) and does not require any numerical optimization which makes it easy to implement on real hardware. It follows the idea to use the heat pump to overheat the existing hot water storage in times of cheap electrical energy (oversupply). This way, converting electrical into thermal energy allows to economically shift electrical loads and hence to react at grid needs. The proposed optimization scheme is evaluated in a simulation study based on the simulation platform TRNSYS. A detailed evaluation of the algorithm in different application scenarios has been conducted by using a comprehensive system model of the investigated solar heat pump system. The evaluation presents the impact of different characteristics of the incentivizing price signal as well as prediction errors onto the load shifting and cost saving potential.**

Keywords – **Heat Pump, Demand Side Management, Load Shifting, Energy Management, Demand Response**

I. INTRODUCTION

Overcoming the problem of the fluctuating provisioning of electrical energy via renewable energy resources is seen as a major challenge of the future electricity grid, and shifting loads on the demand side is one promising solution [27]. Grid-reactive buildings that are able to adjust their local electricity consumption are discussed as important parts of the future energy landscape (e.g. [3], [26], [30]). In this context, heat pumps are very interesting as they are responsible for large parts of the overall electricity consumption in buildings. By converting electrical energy to heat in times of electrical oversupply they offer promising ways for load-shifting; especially in combination with existing thermal storages. As a result, the building has a lower electrical demand in times when the grid requires it.

Different concepts for load shifting with heat pumps are possible. In [22], controls based on grid frequency, energy exchange markets, or via direct commands from the utility are separated. This paper focuses on incentives derived from energy exchange markets where the supply and demand is matched, and reflected in terms of variable prices. If these prices are predicted some hours ahead and are communicated to the end-consumer, an economic stimulus is given to adapt the electrical demand to this signal and therefore to shift the electrical energy consumption (see [31] for an introduction to time variable electricity price tariffs).

The concept of load shifting with heat pumps is visualized in Fig. 1, and a real-world realization of this concept was done within the project Sol2Heat [10]. In the context of a solar heat pump system [6], the project investigated the intelligent scheduling of heat pumps together with household appliances, considering local photovoltaic (PV) systems and variable price tariffs. This paper focuses on the heuristic predictive optimization scheme of the heat pump operation. To evaluate the optimization algorithm in an application-oriented simulation, the program logic (Java code) has been coupled with the simulation platform TRNSYS 17 [14], where a detailed simulation model of the solar heat pump system is available. In addition to the description of the predictive heuristic optimization scheme, this paper includes simulation results based on the solar heat pump system and two different pricing schemes.
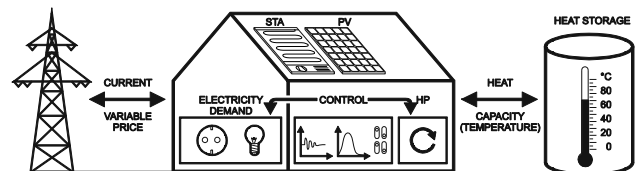
Fig. 1. Visualization of the concept of grid-reactive heat pump operation.

II. RELATED WORK

Grid- or market reactive heat pump operation is a current topic of different research projects (e.g. [1], [4], [9], [10]), and it is already addressed by numerous papers. *Young Jae Yu* [5] presents a model-predictive control (MPC) approach for grid-reactive heat pump operation which uses the building as thermal storage. Different prediction horizons, resulting operative room temperatures, and the share of renewable energies on the heat pump's electricity supply are evaluated. *Loesch et al.* [19] present an evolutionary algorithm for scheduling the heat pump operation based on an external price signal, an external load limitation signal as well as a prediction of local PV generation. The approach is designed to be used within a holistic optimization, which allows to jointly schedule the heat pump with further electrical appliances in the building, such as household devices. In [8], *Faßnacht et al.* present a linear model predictive control (MPC) scheme for the grid-reactive operation of modulating air-to-water heat pumps, where the hot water storage is used as buffer for the

load shifting. In [15], *Oldewuertel et al.* summarize their work on a MPC scheme for building automation control, which takes into account an electrical price forecast. A least-square support vector machine is used to predict the electricity prices, whereas the inputs of the algorithm are prices and grid loads of the last day. A bilinear building model is used and the optimization problem is solved with a Sequential Linear Programming method. In [18], a MPC strategy for buildings is presented by *Vrettos et al.*, where a heat pump, an electrical resistance heater, slab cooling, a PV system and a battery are taken into account. Maximum monetary savings for two price signals via performance bound simulations are presented and the impact of price steps, different length and magnitude are evaluated. In [21], *Tahersima et al.* present a hierarchical MPC scheme which optimizes the flow temperature of a floor heating system, such that the underlying single room controller (PI) in the room with the highest heating load is always working near a 90 % open valve. Beside an ambient temperature forecast, also a price signal forecast is taken into account. In [16], [20], [22], [23], [24] further control methods for heat or cooling supply that take into account dynamic pricing are presented. The feature all the presented strategies have in common is that a numerical optimization is needed in each time step to solve the problem.

In contrast to the above named approaches, this paper introduces a predictive scheme for grid-reactive heat pump operation without the need of a numerical optimization. Hot water storage is used as heat storage capacity.

III. SOLAR HEAT PUMP SYSTEM

The predictive algorithm for heat pump scheduling is realized in the context of a solar heat pump system. Fig. 2 depicts the basic scheme of the system. The core heat generation for the buildings heat and domestic hot water (DHW) demand is supplied by a 7 kW brine/water heat pump. The only heat sources of the heat pump are special flat plate solar thermal collectors, which are equipped with ventilators on the backside of the solar absorber. Therefore, the collector cannot just use solar radiation, but also ambient air to heat the brine in the collector.

The collectors are called solar-thermal-air (STA) collectors in the latter. The system is equipped with a 290 kg ice storage, which is used to store solar energy from the day into the night, to use it as energy source of the evaporator of the heat pump and to smooth the evaporator inlet temperatures. The STA-collectors cannot only supply the heat pump with energy on a low temperature level, but also direct to a stratified hot water tank with heat on a higher temperature level to cover the heat demand for heating and DHW.

The DHW is produced by an inner heat exchanger in the hot water storage. Therefore, the temperature in the upper part is held on a higher temperature level than the middle part of the storage. The generated heat of the heat pump is supplied to the upper part of the hot water storage for DHW and in the middle part of the storage for the heating demand.
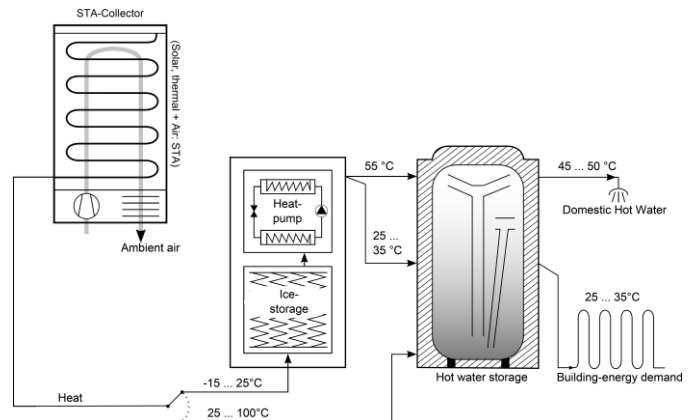
Fig. 2. Conceptual scheme of the solar heat pump system.

In the context of [2] and [7], a detailed model of the solar heat pump system in TRNSYS was developed, which was used in this study to evaluate the proposed heuristic predictive optimization scheme, in an application-related simulation.

IV. PREDICTIVE OPTIMIZATION ALGORITHM

The proposed predictive algorithm is based on the short term forecast (< 1 day; granularity of 1 hour) of the building's heating and domestic hot water demand, the expected energy supply of the STA-collectors to the hot water storage, and the expected surplus electrical energy generated by the optional PV-system. Furthermore, a prediction of the market price is needed. Fig. 3 depicts the inputs and outputs of the proposed algorithm.
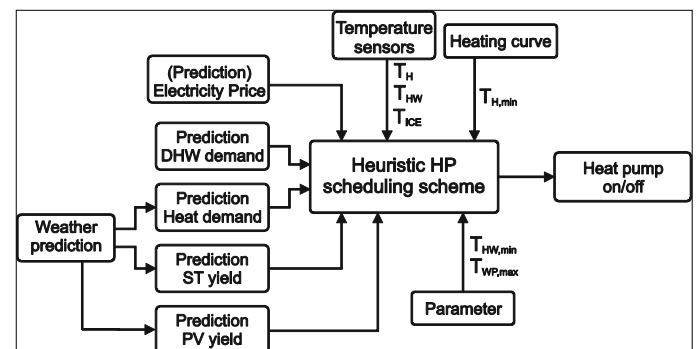
Fig. 3. Inputs and Outputs of the heuristic optimization scheme for heat pump scheduling.

The target of the algorithm is to run the heat pump, so that the operation costs of the system are minimized. This is achieved by running the heat pump in times when the current prices are low and to use the stored energy in the hot water storage when the current prices are high. The hot water storage (see Fig. 2) is a stratified storage with an inner heat exchanger for DHW. The upper part of the storage is held on a higher temperature level than the middle part of the storage to meet the DHW demand. Hence, the algorithm assumes that the system virtually has two storages. Considering a time frame

between *t=now* and *t=now+PredHorizon*, the algorithm decides when to run the heat pump.[1] For this time frame, the runtime of the heat pump is scheduled so that the operating costs are minimized.

The heuristic predictive algorithm can be concretized by the following 10 steps, which are triggered every hour:

1. Read in the actual measurements of the mean temperatures in the upper part T_{HW} (domestic hot water) and lower part T_H (heating water) of the hot water storage, and the temperature of the ice storage T_{ice}.

2. Calculation of the energy amount that is stored in each hot water storage:

$$Q_{HW} = c_{p,water} m_{HW} \left(T_{HW} - T_{HW,\min} \right),\qquad(1)$$

$$Q_H = c_{p,water} m_H \left(T_H - T_{H,\min} \right).\qquad(2)$$

These amounts of energy can be used in the optimization horizon to meet the respective energy demands for DHW and the heating demand, without the need of heat pump operation. $T_{HW,min}$ is a setting value, whereas $T_{H,min}$ can be calculated based on the heating curve and the actual ambient temperature.

3. Calculation of the overall energy demand for the respective storage (DHW and heating demand) in the optimization horizon, which has to be met by the heat pump operation. This is based on the predicted heat demand of the building $Q_{H,pred}$, the predicted DHW demand $Q_{HW,pred}$, the predicted solar thermal yield in the hot water storage $Q_{ST,pred}$, and the already stored energy in the storages Q_{HW} and Q_H (see step 2).

$$Q_{HP,HW} = Q_{HW,pred} - Q_{HW} - Q_{ST,pred}\gamma\qquad(3)$$

$$Q_{HP,H} = Q_{H,pred} - Q_H - Q_{ST,pred}(1-\gamma)\qquad(4)$$

At this γ is a constant factor that divides the solar thermal energy yield in the upper part and the lower part of the hot water storage (when the hot water storage is charged directly by the STA-collectors, always the upper and the lower part are affected simultaneous).

4. Approximation of the heat pump efficiency based on the actual measurement data. The heat pump coefficient of performance is calculated based on the Carnot cycle efficiency adapted by a constant[2]:

$$COP_{HP,HW} = \eta_{C,HP} \frac{T_{HW}}{T_{HW} - T_{ice}} \ ,\qquad(5)$$

$$COP_{HP,H} = \eta_{C,HP} \frac{T_H}{T_H - T_{ice}} \ .\qquad(6)$$

At this $\eta_{C,HP}$ is the quality grade of the heat pump that takes the deviations of the real heat pump cycle to the ideal Carnot cycle into account.

5. Calculation of the overall needed runtime of the heat pump in the optimization horizon. This takes the energy demand that has to be met by the heat pump (see step 3) and the efficiency of the heat pump (step 4) into account. The latter is assumed as constant over the optimization horizon:

$$t_{HP,HW} = \frac{Q_{HP,HW}}{COP_{HP,HW} P_{el,HP}} \ ,\qquad(7)$$

$$t_{HP,H} = \frac{Q_{HP,H}}{COP_{HP,H} P_{el,HP}} \ .\qquad(8)$$

The electrical energy demand of the heat pump compressor $P_{el,HP}$ is also assumed as constant over the optimization horizon.

6. Calculation of the number of timeslots needed for the heat pump operation within the optimization horizon. In this study the length of the timeslots was chosen to be 15 minutes because of two reasons: This equals the sampling rate of the price signal and further results in a minimum heat pump runtime of 15 minutes, whereby, according to [29], efficiency losses due to cyclic operation of the heat pump can be neglected.

$$Slots_{HW} = \frac{t_{HP,HW}}{15\,[\min]}\qquad(9)$$

$$Slots_H = \frac{t_{HP,H}}{15\,[\min]}\qquad(10)$$

7. Calculation of the costs of *each* timeslot in the optimization horizon, which *would* be caused by the heat

---

[1] In this study predictive horizons of 9 h and 24 h have been used (see section VII). But this is not an invariable rule in the algorithm.

[2] Note: This calculation could also be based on polynomial curves based on measurements of the heat pump (heat pump characteristic curves).

pump when running in this timeslot. This calculation takes the electrical power demand of the heat pump $P_{el,HP}$ (assumed as constant), the electrical price for this timeslot c_k, the PV surplus of local energy generation after meeting the household demand $PV_{s,k}$ and eventually a tariff for feed-in compensation s_k into account. The cost calculation for the slot is divided in two steps.

At first, for each time slot the external electrical energy needed from the grid ($P_{grid,HP,k}$) and the self-consumption of PV ($P_{SC,HP,k}$) is calculated:

$$P_{grid,HP,k} = MAX(P_{el,HP} - PV_{s,k}, 0), \tag{11}$$

$$P_{SC,HP,k} = MIN(PV_{s,k}, P_{el,HP}) \tag{12}$$

Second, the costs for the respective timeslot k are calculated:

$$C_{Slot,k} = P_{grid,HP,k} \cdot c_k \cdot \Delta t - P_{SC,HP,k} \cdot s_k \cdot \Delta t . \tag{13}$$

The self-consumption of PV is taken into account since generated electrical energy that is not sold to the grid is related to costs due to the loss of feed-in compensation (opportunity costs).

8. Long-term optimization: In step **7**, the prices for running the heat pump in each timeslot within the optimization horizon are calculated. This results in a two column matrix of length N with the time slot number within the horizon in one column and the cost of heat pump operation in the other column. This matrix is sorted ascending according to costs. Afterwards, the third column is introduced, indicating the status of the heat pump within the respective time step. The heat pump status within this column can either be *HP_off* (initial default value), *HP_DHW* or *HP_HEATING*. Starting with the cheapest slot, the heat pump status is then alternatingly set to *HP_DHW* and to *HP_HEATING* as long as the number of the already chosen slots is smaller as the number of the needed slots within the optimization horizon (see step 6, $Slots_{HW}$ and $Slots_H$). The status signals till the next re-optimization are saved and used for switching the heat pump system.

9. Short-term optimization: After each long-term optimization, a short-term optimization considering a smaller optimization horizon is conducted. The proceeding of the two moving horizons for the long- and the short-term optimization is depicted in Fig. 4 (exemplary prediction horizon lengths). The illustration assumes a long-term optimization horizon of 5 hours (N=20) and a short-term optimization horizon of 1 hour (M=4).
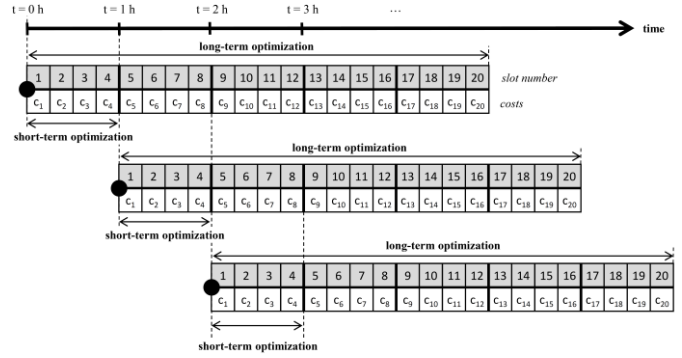
Fig. 4. Moving optimization horizon with a long- and short-term optimization (exemplary prediction horizon length).

The short-term optimization is introduced to also consider and shift the runtimes of potential forced starts, which are triggered, when the minimum temperature is reached. For both storages, it checks, whether the heat pump status signal is set to run for the respective storage within the next *M* time slots. If the heat pump is not running for the respective storage, it calculates whether its minimum temperature will be undershot within the next *M* timeslots based on the current storage temperature and the related demand prediction. If the minimum temperature is predicted to be undershot, so when

$$T_H - \frac{Q_{H,pred,short}}{c_{p,water} m_H} < T_{H,min}, \tag{14}$$

or

$$T_{HW} - \frac{Q_{HW,pred,short}}{c_{p,water} m_{HW}} < T_{HW,min}, \tag{15}$$

the heat pump's status is set to run for the respective storage in the cheapest timeslot within the next M slots, independent of the prior long-term optimization (i.e. the status signal is set to *HP_HEATING* or *HP_DHW*). First, this is done for the heating water storage, and then for the DHW storage. At this, the latter does not overwrite the first; if the short-term optimization resulted in the heat pump running for heating water, then the slot which in the short-term optimization potentially is used for the DHW storage, is the second cheapest one. Priority is given to the heating water storage, since it is responsible for the largest part of the overall heat pump runtime demand.

10. The minimum and maximum allowed temperatures in the heating water and domestic hot water storage are supervised continuously. When the minimum temperature in a water storage is undershot, the heat pump immediately starts to run for the respective storage, and when the maximum temperature is overshot, the heat pump immediately stops to run for the respective storage till the end of the current slot. The minimum temperature of the domestic hot water storage is a setting value (43 °C in this study), whereas the minimum temperature in the heating storage is calculated

by the heating curve minus a hysteresis (2 K in this study). The maximum temperature is a setting value for both storages. In this study it is set to 57 °C for the domestic hot water part and to 55 °C for the heating water part of the storage.

V. REQUIRED FORECAST MODELS

As illustrated in Fig. 3, the predictive algorithm uses short-term predictions of the heating water demand, the domestic hot water demand, and the electrical household demand, the solar thermal yield in the hot water storages, and the electrical supply of the local PV system. Prediction models for all these values have been developed and investigated within the project Sol2Heat. At this, the forecast models of the demand side (heating and DHW demand, electrical household demand) and the solar thermal yield model have the same basic structure: A matrix is set up, in which the measured recursive mean value of the relevant variable is saved. For the DHW prediction, e.g., the matrix is divided into $j = 7$ parts for each day of the week, and into $i = 96$ parts for each 15 minute slot of the respective day. The matrix is filled with the measured (heat meter) mean value of the DHW demand in the past for each combination of day (i) and time of day (j):

$$\begin{pmatrix} \overline{Q}_{1,1} & \cdots & \overline{Q}_{1,j} \\ \vdots & \ddots & \vdots \\ \overline{Q}_{i,1} & \cdots & \overline{Q}_{i,j} \end{pmatrix} \qquad (16)$$

The mean value of the respective measured variable in equation 16 is further recursively adapted after each new measurement:

$$\overline{Q}_{i,j,new} = \xi\overline{Q}_{i,j,old} + (1 - \xi)Q_{actual} \qquad (17)$$

At this, ξ is a weighting factor in the range [0,1] which balances the weight of the historical and newly measured values. The resulting matrix is then used for the predictions. For the prediction of the PV yield, a static model based on results of the standard collector tests has been developed.

In this study perfect prediction data is used for the basis cases. In the second step, the impact of forecast deviations on the simulation results is evaluated.

VI. INCENTIVIZING PRICE SIGNALS

Two different price signals have been used in this simulation study: (1) A fully market driven price signal based on the German EPEX Intraday 15 minute spot prices [11], and (2) a price signal based on a real German tariff. For the latter, two different variations have been investigated (tariff as offered today vs. same tariff complemented by variations of the Germany EPEX Intraday spot prices which are directly forwarded to the customers).

A. Pure Market Driven Price Signal (MDPS)

This price tariff is based on the EPEX Intraday 15 minutes spot prices in Germany 2014. Therefore, the 15 minute Intraday prices between 01/01/2014 and 11/08/2014 have been extracted from [11]. To get a one year period, the extracted profile has been duplicated, linked together and appropriately cut. The prices of the resulting one year profile have been multiplied by 10, which results in a price signal with an *assumed* mean value of 31.85 €cent/kWh and a standard deviation of 20.1 €cent/kWh. Fig. 5 depicts the histogram of the generated price signal. The price signal reflects the fluctuations of the German 15 minute Intraday market, but the mean height of the price is assumed. This price signal was used in this study as a theoretical example to evaluate the potential for savings with price signals of high variance.
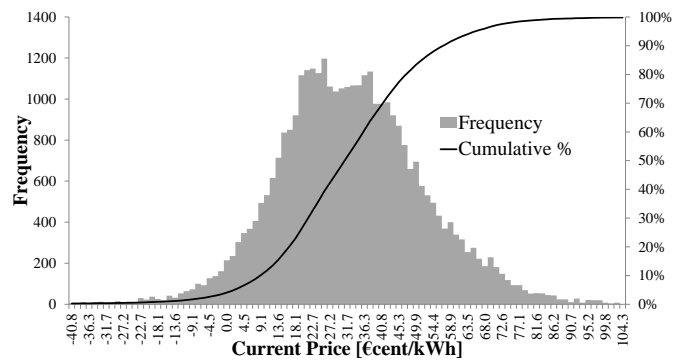
Fig. 5. Histogram of the assumed market driven price signal (MDPS).

It has to be noted that a price signal like that can only be realized when the actual static costs of the electricity price would also be coupled according to the supply and demand balance at the electrical energy exchange market (whereby they would also vary in time, dependent on the market). In Germany these static costs mainly consist of grid fees, apportionments according to the Renewable Energy Act (EEG) as well as the Combined Heat and Power Act (KWKG), taxes, and concession fees (see e.g. [28]).

B. Real Price Signal based on a today existing tariff (RPS)

The basis of this tariff is a real available electricity tariff for heat pumps and household demands in Germany. [3] The tariff is separated into a high and a low tariff part.

TABLE I

HIGH AND LOW TARIFF PART OF THE REAL TARIFF [13]

TIME	PRICE
22:00-06:00	17.32 €cent/kWh
Otherwise	25.32 €cent/kWh

Two cases of this tariff have been investigated: First, exactly the tariff as offered today (*RPS-constant*). This allows

---

[3] *Casa XL tariff* of the supplier Energiedienst AG (www.energiedienst.de). The static yearly base price of this tariff has been neglected. Just the consumption price has been taken into account.

evaluating the potential of the algorithm in a realistic context. Second, the basis tariff supplemented by the variations of the EPEX Intraday 15 minute spot prices (*RPS-fluctuating*). This corresponds to a forwarding of the energy exchange market fluctuations to the customer. Therefore, the basic price signal in Table I is adapted according to the following formula:

$$c_k = c_{k,Basic} + F \cdot c_{k,Intraday} - F \cdot \overline{c}_{k,Intraday} \qquad (18)$$

where c_k is the resulting cost in the actual time step, $c_{k,Basic}$ the cost of the tariff in Table I, $c_{k,Intraday}$ the actual cost of the Intraday spot market, $\overline{c}_{k,Intraday}$ the mean costs and F a factor for justifying the fluctuations of the resulting signal (in this study F=1 has been used). Fig. 6 depicts the histogram of the derived price signal.
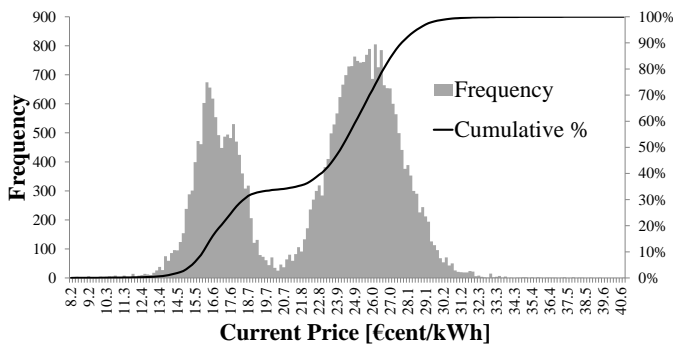
Fig. 6. Histogram of the price signal based on a real tariff supplemented by variations of the 15 minute Intraday spot market (RPS-fluctuating, F=1).

The mean value of the adapted RPS (*RPS-fluctuating*) is the basic tariff itself (*RPS-constant*). The adapted RPS results in overall much lower fluctuations than the MDPS.

VII. SIMULATION RESULTS

The system model of the solar heat pump system described in Section II has been modeled in the simulation platform TRNSYS 17 [14]. The predictive optimization algorithm described in Section III has been implemented in Java and is currently being ported to a hardware controller regulating the solar heat pump system. In order to evaluate the algorithm in different scenarios, a new TRNSYS type for coupling the simulation platform with the Java-based program logic has been developed and published open-source [12].

At first, three reference simulations (different heating demands) have been realized with the standard control. Standard control means that recharging of both the upper and the middle part of the hot water storage via the heat pump is controlled by a standard hysteresis control, whereby priority is given to the DHW storage. In all simulations the boundary conditions in Table II have been used. The heat demands as well as the hot water tapping were read as time series.

TABLE II
BOUNDARY CONDITIONS OF THE REFERENCE SIMULATIONS

CONDITION	VALUE
Weather data	Würzburg, Germany[4]
DHW demand	2000 kWh (45 °C)
Heating demand	5462 / 7281 / 9047 kWh
Heating curve	35 °C / 30 °C
STA-collectors	5 / 11.45 m²
Nom. heat pump power	7 kW
Hot water storage	1000 l
Ice storage	290 kg

For the simulations with the RPS, the long term optimization horizon was set to 9 h and the short term horizon to 2 h, whereas in the simulations with the MDPS the optimization horizons were set to 24 h and 5 h. A good choice of the horizons proved to be dependent on the price signal.
Table III summarizes some results of the simulations with the standard hysteresis-based control (with RPS1=*RPS-constant*, RPS2=*RPS-fluctuating*).

TABLE III
SELECTED RESULTS OF THE REFERENCE SIMULATIONS

HEATING DEMAND [kWh/a]	DHW YIELD [kWh/a]	SHP EL. DEMAND[5] [kWh/a]	COST WITH MDPS/RPS1/RPS2 [€/a]
5462	1991	1880	575 / 413 / 412
7281	1988	2475	751 / 537 / 535
9047	1987	3041	915 / 656 / 656

A. Simulation results with the market driven price signal (MDPS)

Fig. 7 depicts simulation results of an example day in January based on the standard control. It can be seen that the heat pump operation is independent of the price signal and is purely heat demand driven. The heat pump is running so that the storage temperatures are kept between the minimum and maximum temperature.
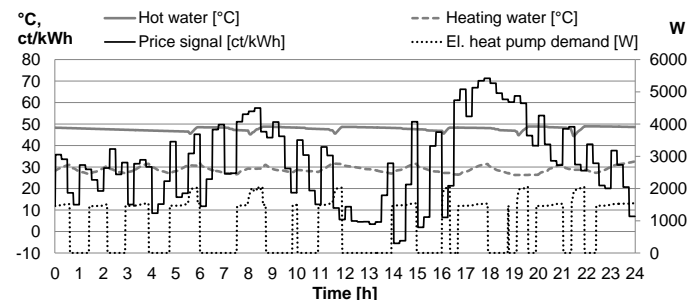
Fig. 7. Simulation results of an example day in January with the standard control (hot water = upper part and heating water = lower part of the hot water storage[6]).

---

[4] Note: The weather data is taken from the Meteonorm dataset [25], which is a generated profile. This means that the weather data and the price signal are not of the same year. It is assumed that the effect on the simulation results is relatively low as of today. Nevertheless, in future work weather data and price signal should be of the same period to evaluate their mutual influence.
[5] The whole system, exclusive the heat distribution and the condenser circle pump have been taken into account.

Fig. 8 depicts simulation results of the same day, but with the predictive control of the heat pump presented in chapter III.
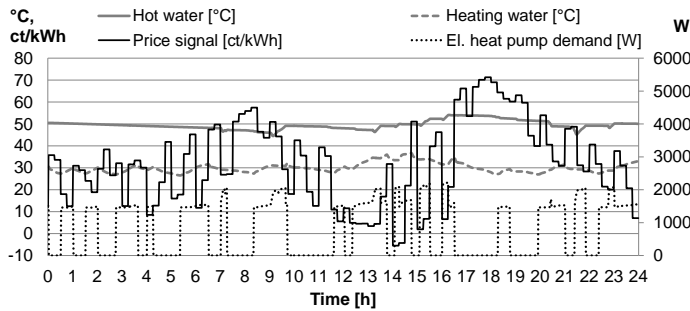
Fig. 8. Simulation results of an example day in January with the predictive control using the MDPS.

Now the heat pump operation is shifted to the low price valleys most of the time. Sometimes the heat pump runs when the temperature boundaries in the hot water storage are violated[7] (e.g. between 18 and 19 o'clock). Between 12 and 16 o'clock the hot water storage is superheated to bridge the following high-price period.

Fig. 9 depicts the operation costs with the MDPS, and Fig. 10 – the achieved operation cost reduction of the solar heat pump system in the simulations.
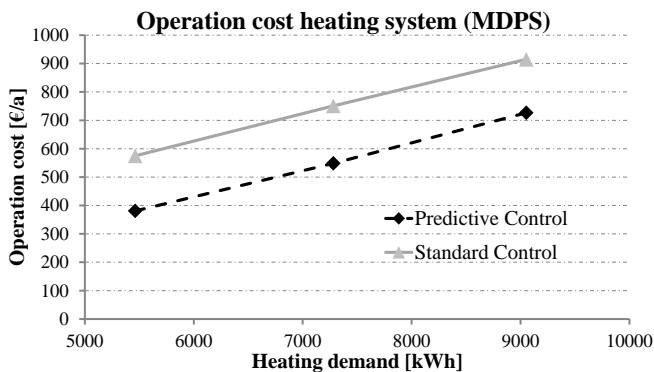
Fig. 9. Operation costs of the solar heat pump system using the MDPS.

It can be seen that with a rising heat demand, the relative reduction potential gets lower. This is due to the fact that in cases of a higher heat demand, the heat pump has to run longer times and therefore the shifting potential is diminished. Then, the heat pump more often has to run in high price times in order to satisfy the building's heat demand.
This effect is mainly influenced by the fraction of the heat pump power and the building's heating load. With rising heat pump power and constant heating load of the building, the shifting potential grows. This means that the results (cost reduction potentials) in this paper are just valid for the combination of the solar heat pump system and the building loads, and that they cannot be generalized. It further connotes

that oversized dimensioning of heat pumps is beneficial for Demand Side Response. Finally, it is worth mentioning that potential analyses investigating the effect of load shifting with heat pumps onto the market and/or grid have to take into account that in cold temperature periods a significant amount of heat pumps are (nearly) not available for load shifting, due to high needed runtimes to meet the heat demand of the building.
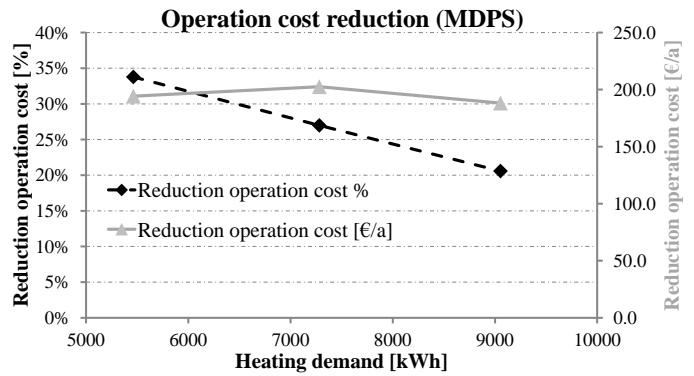
Fig. 10. Reduction in operation costs for the solar heat pump system with the optimized control using the MDPS.

Fig. 11 depicts the electrical energy demand of the solar heat pump system with the standard and the predictive control. With the predictive control, the electrical demand of the heating system itself increases (between 2 % - 6 %). This is mainly caused by efficiency losses of the heat pump due to higher system temperatures through overheating of the hot water storage.
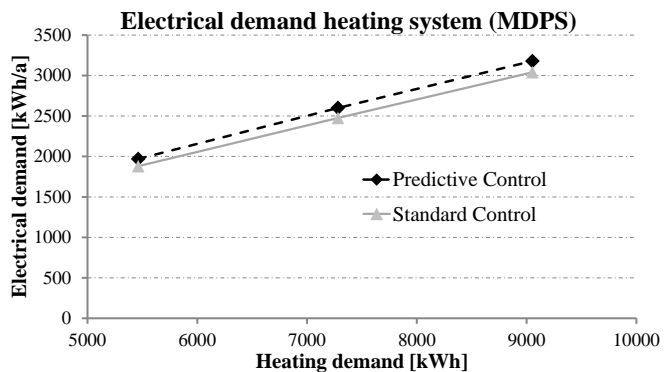
Fig. 11. Electrical demand of the solar heat pump system with the standard and the predictive control using the MDPS.

B. Simulation results with the signal based on a real tariff (RPS)

Fig. 12 depicts simulation results of a day in January with the predictive control and the adapted *RPS-fluctuating*.[8] As in Fig. 8, it can clearly be seen that the heat pump mileages are shifted to the low price valleys. It also can be seen that the price fluctuations with the adapted *RPS-fluctuating* are much lower than of the MDPS.

---

[6] Both temperatures are mean values in this part of the tank. The heating flow temperature therefore is higher than the depicted storage temperature.
[7] See chapter III point 10 of the algorithm.

[8] Different day as in Fig. 7 and Fig. 8.
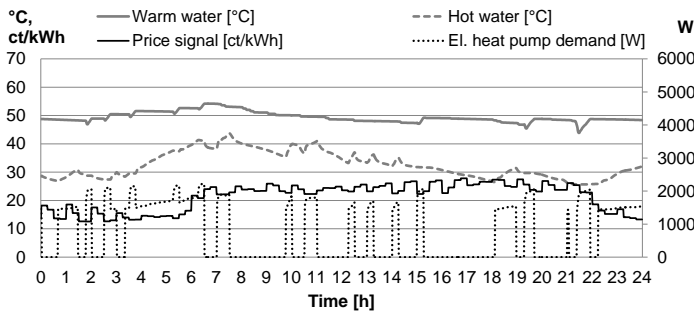
Fig. 12. Simulation results of an example day in January with the predictive control using RPS-fluctuating.

In the morning with a longer low price period the temperatures in the upper and the lower part of the hot water storage are superheated to utilize the tariff. This leads to storage losses and efficiency losses of the heat pump, due to higher operating temperatures. This effect, in combination with the relative small fluctuations of the price signal, results in overall much lower savings for the end consumers. Fig. 13 depicts the simulated operation cost and shows that the predictive control outperforms the standard control for all demand scenarios (cost difference from standard to predictive control between 3.8 to 7.4 %). It also can be seen that in case of the standard control, nearly no difference between the RPS variants can be observed. Hence, the comparisons in the latter are all realized with the standard control - RPS constant / Predictive control - RPS-fluctuating combination.
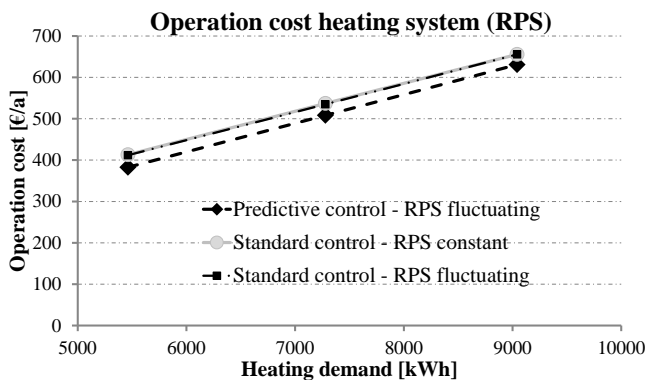
Fig. 13. Operation costs for the solar heat pump system with the standard and the predictive control using both RPS variants.
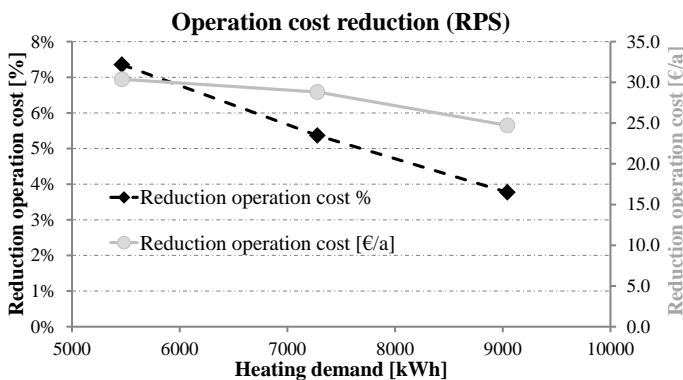
Fig. 14. Reduction in operation costs for the solar heat pump system with the optimized control using RPS -fluctuating .

Fig. 14 shows the operation cost reduction of the simulations using the *RPS-fluctuating*. As already described for the MDPS scenario, it can be seen that a higher heating demand also decreases the percentage operating cost reduction since the ability to utilize price valleys is minimized.

Although the savings here are small, the goal of the adaptation of the heat pump operation to the grid signal is fully achieved. If in practical applications a price signal with higher fluctuations cannot be realized, an alternative way to compensate the end consumer for their adaptation could be bonuses for heat pumps which provide this mechanism.

C. Influence of the prediction accuracy

For the proposed predictive algorithm, predictions of the heat and hot water demand and of the solar thermal demand[9] are used. By now perfect prediction data have been used. To evaluate the influence of the prediction accuracy on the control performance of the predictive controller, simulations with disturbed prediction data have been conducted.

Fig. 15 depicts the operation cost reductions in dependence of the prediction error of the heating demand. For the simulations, the perfect prediction demand was supplemented by a static error. At this, the incorrect prediction for each time step is calculated by:

$$\hat{Q}_{error,t} = \hat{Q}_{perfect,t} \cdot (1 + error). \qquad (19)$$

In Fig. 15 it can be seen that when a lower heat demand is predicted as actually occurred in reality, the reduction of the operation costs decreases. This can be explained by the fact that the hot water storage is not superheated enough in high price times so that the heat pump has to run at high costs due to approaching violations of the minimal allowed hot water storage temperatures.
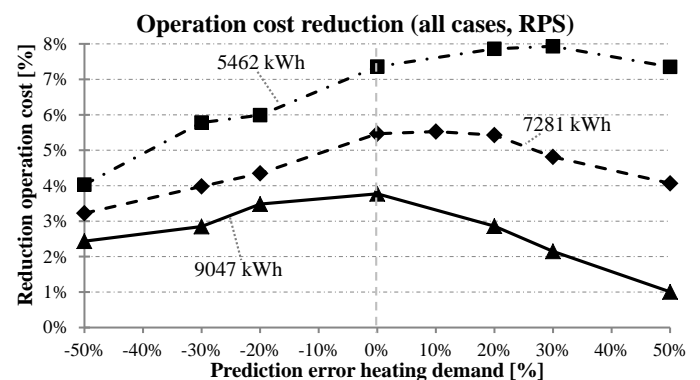
Fig. 15. Reduction in operation costs for the three evaluated heat demands in dependence of the static prediction error (predictive control using RPS-fluctuating).

In the two cases with lower heat demand, a higher predicted heat demand than actually needed leads at the beginning to an

---

[9] Simulations with an additional electric PV system have not been conducted in this study.

increase in savings. This can be explained by an improved usage of the variable price tariff, and indicates still possible improvements for the heuristic. One reason for that is that storage losses are at the moment not accounted for in the algorithm, whereby the heat pump always produces slightly less heat as finally needed. However, in case of the 9047 kWh yearly heat demand, the saving potential immediately decreases with wrong predictions.

Fig. 16 depicts the operation cost reduction in dependence of the static error of the heat demand prediction, now for the simulations with the MDPS. The results show qualitatively the same behavior.
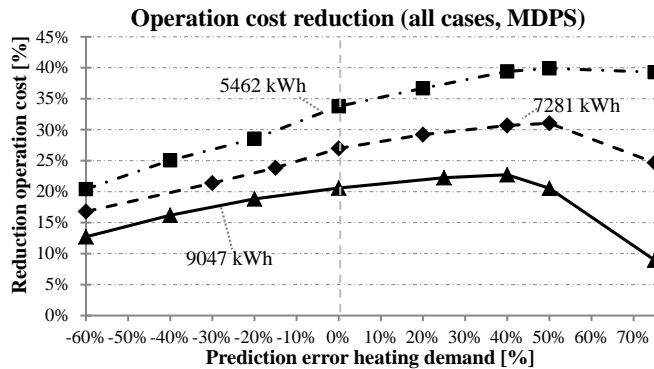
Fig. 16. Operation costs reduction for the three evaluated heat demands in dependence of the static prediction error (MDPS; connection between points just for visualization).

In summary it can be stated that the influence of wrong predictions on the simulation results is low and that with a large constant prediction error of 50 %, in all investigated cases savings still could be achieved.

So far we investigated the impact of constant prediction errors with a *constant* deviation of ± x %. In addition to this, the impact of a *random* error according to a predefined standard deviation based on the perfect prediction is investigated. A random prediction error means that randomly either a too high or a too low demand is predicted, whereby predictions of demands lower than 0 are excluded. A too high prediction results in overproduction of thermal energy which in turn results in an inefficient consumption of the electrical energy, and a too low prediction results in inability to schedule the heat pump to price valleys.

Fig. 17 shows the impact of random prediction errors onto the operation cost. The x-axis describes the percentage size of the prediction error based on the perfect prediction by means of the coefficient of variation of the introduced random error.

At this, the coefficient of variation is calculated by the standard deviation of the prediction error divided by the mean hourly heat demand (in the heating season):

$$CV = \frac{\sigma_{prediction}}{Q_H} \; [\%] \; . \tag{20}$$
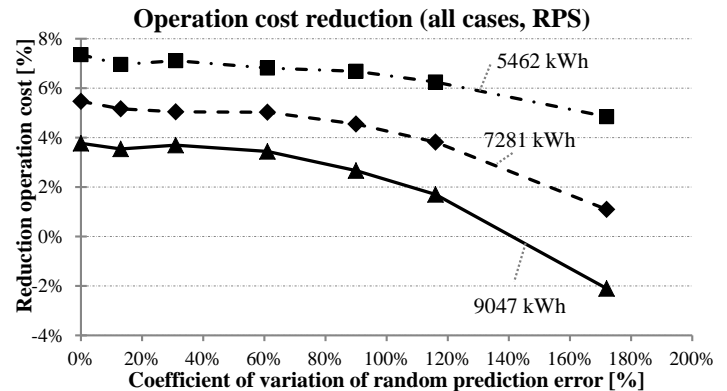
Fig. 17. Operation cost reduction in dependence of the random prediction error (connection between points just for visualization).

Table IV depicts the standard deviation for different coefficients of variation and different yearly heat demands.

TABLE IV

Sᴛᴀɴᴅᴀʀᴅ ᴅᴇᴠɪᴀᴛɪᴏɴꜱ σ ᴏꜰ ᴛʜᴇ ʀᴀɴᴅᴏᴍ ᴘʀᴇᴅɪᴄᴛɪᴏɴ ᴇʀʀᴏʀꜱ

CV [%]	5462 [kWh/a]	7281 [kWh/a]	9047 [kWh/a]
13 %	0.2 kWh	0.16 kWh	0.12 kWh
31 %	0.49 kWh	0.39 kWh	0.29 kWh
61 %	0.98 kWh	0.78 kWh	0.59 kWh
90 %	1.44 kWh	1.15 kWh	0.86 kWh
116 %	1.9 kWh	1.5 kWh	1.12 kWh
172 %	2.74 kWh	2.19 kWh	1.65 kWh

In Fig. 17 it can be recognized that the operation cost reduction decreases with an increased random prediction error for the heat demand. However, the influence of the random prediction error onto the saving potential is small. Significant effects can only be observed at errors higher 100 % (CV). The proposed algorithm, therefore, seems to be robust against the prediction quality.

VIII. Sᴜᴍᴍᴀʀʏ ᴀɴᴅ Oᴜᴛʟᴏᴏᴋ

In this paper a heuristic predictive optimization scheme for grid-reactive heat pump scheduling is proposed. The algorithm is realized without the need of any numerical optimization and can therefore be realized easily and with low computing capacity. The algorithm is evaluated in combination with a real solar heat pump system. A simulation study is presented, in which the heat pump shifting is proved qualitatively. Furthermore, saving potentials for different assumed price signals have been quantified.

It was shown why the shifting potential of the individual system depends on the ratio between the heat pump power and the building's heating load. Therefore, the presented results cannot be generalized. In further steps, results in dependence

of a dimensionless number describing this ratio should be generated to get more generalizable results. Furthermore, in future work the weather data should be of the same time period as the price signal because the first has influence on the second.

Finally, an analysis of the effect of prediction errors that are used as input for the algorithm was provided. It was presented that prediction errors of the building's heat demand result in small effects on the results of the predictive control. Even with very high errors (± 50 %), savings still could be achieved. The next step in this context is the evaluation of combinations of errors for different predictions (heating demand, DHW, and solar thermal yield).

IX. ACKNOWLEDGMENT

REFERENCES

[1] G. Andersson, E. Vrettos and S. Koch, "SmartGrid-Polysun Design Tool for Local Load Management," ETH Zürich, Power Systems and High Voltage Laboratories (EEH), Switzerland, Annual Report, 2013.

[2] S. Asenbeck, H. Drück, S. Bachmann, H. Kerskes, H. Müller-Steinhagen, "Simulationsstudie Solar-Wärmepumpensystem zur Trinkwassererwärmung und Raumheizung," University of Stuttgart, Institute of Thermodynamics and Thermal Engineering, Tech. Rep. 2008, unpublished.

[3] C. Nabe et al. "Potenziale der Wärmepumpe zum Lastmanagement im Strommarkt und zur Netzintegration erneuerbarer Energien," Ecofys Germany GmbH and Prognos AG , Germany, Final Report, 2011.

[4] S. Pfaffen and K. Werlen, "WARMup Optimale Verwertung der Flexibliität von thermischen Speichern," Misurio AG, Switzerland, Final Report, 2013.

[5] Y. J. Yu, "Demand-Side-Management with Heat Pumps for Single Family Houses," 13th Conference of International Building Performance Simulation Association, Chambery, France, 2013, August 26-28.

[6] U. Leibfried, "Integrierte Systemlösungen für Bestand und Neubau zum Erreichen der Klimaziele" presented at 21th Symposium on thermal Solar Energy, Bad Staffelstein, Germany, 2011.

[7] T. Faßnacht "Moderne Regelungsansätze für Solarsysteme mit integrierter Wärmepumpe zur Gebäudeheizung," PhD Thesis (Manuscript; to be published), University of Stuttgart, Germany, 2015.

[8] T. Faßnacht, A. Abdul-Zahra and A. Wagner, "Modellbasierte prädiktive Regelung für Wärmepumpen zur Integration von Photovoltaik und dynamischen Strompreisen," in *Lüftung/Klima Heizung/Sanitär Gebäudetechnik HLH*, Vol. 5, 2014 , pp. 18-24.

[9] Project Netzreaktive Gebäude, "Verbundvorhaben Netzreaktive Gebäude - Ganzheitliche Bewertung von Bauphysik und Gebäudeenergiesystemen einschließlich ihrer Rolle in der Energiewirtschaft - Energie, Exergie, Leistungsbezug und -abgabe," [Online]. Available: http://www.netzreaktivegebaeude.de/ . [Accessed December 08, 2014].

[10] Project Sol2Heat, "Intelligent creation and storage of solar heat and current for the realization of high solar fractions and for demand side response," [Online]. Available: http://fbta.ieb.kit.edu/182_557.php . [Accessed December 08, 2014].

[11] EPEX SPOT SE, "European Power Exchange," 2014 [Online] Available: www.epexspot.com/de/ [Accessed December 08, 2014].

[12] TRNSYS - Java Coupler, "A TRNSYS type that allows for a bi-directional communication with Java," 2013 [Online]. Available: http://sourceforge.net/projects/trnsys-java-coupler/. [Accessed December 08, 2014].

[13] Energiedienst AG, [Online]. Available: www.energiedienst.de [Accessed December 08, 2014].

[14] TRNSYS 17, "A Transient System Simulation Program," The Solar Energy Laboratory, University of Wisconsin -Madinson, 2012.

[15] F. Oldewuertel, A. Ulbig, A. Parisio, G. Andersson, M. Morari, "Reducing Peak Electricity Demand in Building Climate Control using Real-Time Pricing and Model Predictive Control," 49th IEEE Conference on Decision and Control, Atlanta, USA, December 15-17, 2010. http://dx.doi.org/10.1109/cdc.2010.5717458

[16] Y. Zong, D. Kullmann, A. Thavlov, O. Gehrke, H. W. Bindner, "Active Load Management in an Intelligent Building Using Model Predictive Control Strategy," IEEE PES Trondheim Power Tech, Norway, June 19-23, 2011. http://dx.doi.org/10.1109/ptc.2011.6019347

[17] Y. Zong, D. Kullmann, A. Thavlov, O. Gehrke, H. W. Bindner, "Application of Model Predictive Control for Active Load Management in a Distributed Power System with High Wind Penetration," in *IEEE Transactions on Smart Grid*, Vol. 3, No. 2, June 2012, pp. 1055-1062. http://dx.doi.org/10.1109/TSG.2011.2177282

[18] E. Vrettos, K. Lai, F. Oldewuertel, G. Andersson "Predictive Control of Buildings for Demand Response with Dynamic Day-ahead and Real-time Prices," in *Proceedings of IEEE European Control Conference (ECC)*, 17-19 July 2013, Zürich, pp. 2527-2534.

[19] M. Loesch, D. Hufnagel, S. Steuer, T. Faßnacht, H. Schmeck "Demand Side Management in Smart Buildings by Intelligent Scheduling of Heat Pumps, " IEEE PES International Conference on Intelligent Energy and Power Systems (IEPS), Kyiv, Ukraine, June 2-6, 2014. http://dx.doi.org/10.1109/ieps.2014.6874181

[20] Y. Ma, F. Borrelli, B. Hencey, B. Coffey, S. Bengea and P. Haves, "Model Predictive Control for the Operation of Building Cooling Systems," in *IEEE Transactions on Control Systems Technology*, Vol. 20, No. 3, May 2012 , pp. 796-803. http://dx.doi.org/10.1109/TCST.2011.2124461

[21] F. Tahersima, J. Stoustrup, H. Rasmussen and S. A. Meybodi, "Economic COP Optimization of a Heat Pump with Hierarchical Model Predictive Control," in *Proceedings of 51st IEEE Annual Conference on Decision and Control (CDC)*, 10-13 Dec. 2012 , pp. 7583-7588. http://dx.doi.org/10.1109/cdc.2012.6425810

[22] R. Halvgaard, N. K. Poulsen, H. Madsen, J. B. Jorgensen, "Economic Model Predictive Control for building climate control in a Smart Grid," IEEE PES Innovative Smart Grid Technologies (ISGT), Washington DC, United States of America, 16-20 Jan. 2012.

[23] T. S. Pedersen, P. Andersen, K. M. Nielsen, H. L. Starmose, P. D. Pedersen, "Using Heat Pump Energy Storages in the Power Grid," in *Proceedings of IEEE International on Control Applications (CCA)*, 28-30 September 2011, Denver, CO, USA, pp. 1106-1111. http://dx.doi.org/10.1109/cca.2011.6044504

[24] M. U. Kajgaard, J. Mogensen, A. Wittendorf, A. T. Veress, B. Biegel, "Model Predictive Control of Domestic Heat Pump," in *Proceedings of IEEE American Control Conference (ACC)*, 17-19 June 2013, Washington, DC, USA, pp. 2013-2018. http://dx.doi.org/10.1109/acc.2013.6580131

[25] Meteotest, "Meteonorm Version 6.0, Global Meteorological Database, Software and Data for Engineers, Planners and Eductation," www.meteonorm.com [Accessed December 08, 2014]

[26] N. J. Hewitt, "Heat pumps and energy storage - The challenges of implementation," in *Applied Energy (2012), Nr. 89*, pp. 37-44. http://dx.doi.org/10.1016/j.apenergy.2010.12.028

[27] P. Palensky, D. Dietrich, "Demand Side Management: Demand Response, Intelligent Energy Systems, and Smart Loads," in *IEEE Transactions on Industrial Informatics*, Vol. 7, No. 3, August 2011, pp. 381-388. http://dx.doi.org/10.1109/TII.2011.2158841

[28] DIHK - Deutscher Industrie- und Handelskammertag Berlin | Brüssel: "Faktenpapier Strompreise in Deutschland 2014," February 2014

[29] M. Uhlmann, S. Bertsch, "Dynamischer Wärmepumpentest Phasen 3 und 4," Research Report, Bundesamt für Energie BFE, Switzerland, 29 December 2010.

[30] S. Kreutz, H.-J. Belitz, C. Rehtanz, "The impact of demand side management on the residual load," IEEE PES Innovative Smart Grid Technologies Conference Europe (ISGT Europe), Gothenburg, Sweden, 11-13 Oct. 2010.

[31] A, Ulbig, G. Andersson, "Towards variable end-consumer electricity tariffs reflecting marginal costs: A benchmark tariff," 7th International Conference on the European Energy Market (EEM), Madrid, Spain, 23-25 June 2010. http://dx.doi.org/10.1109/eem.2010.5558777